Purinergic Signalling (2019) 15:375–385
https://doi.org/10.1007/s11302-019-09664-3

ORIGINAL ARTICLE

Selective deletion of ENTPD1/CD39 in macrophages exacerbates biliary fibrosis in a mouse model of sclerosing cholangitis

Sonja Rothweiler[1] · Linda Feldbrügge[1,2] · Zhenghui Gordon Jiang[1] · Eva Csizmadia[1] · Maria Serena Longhi[1] · Kahini Vaid[1] · Keiichi Enjyoji[1] · Yury V. Popov[1] · Simon C. Robson[1]

Received: 18 November 2018 / Accepted: 4 June 2019 / Published online: 26 June 2019

Abstract

Purinergic signaling is important in the activation and differentiation of macrophages, which play divergent roles in the pathophysiology of liver fibrosis. The ectonucleotidase CD39 is known to modulate the immunoregulatory phenotype of macrophages, but whether this specifically impacts cholestatic liver injury is unknown. Here, we investigated the role of macrophage-expressed CD39 on the development of biliary injury and fibrosis in a mouse model of sclerosing cholangitis. Myeloid-specific CD39-deficient mice (LysMCre*Cd39*$^{fl/fl}$) were generated. Global CD39 null (*Cd39*$^{-/-}$), wild-type (WT), LysMCre*Cd39*$^{fl/fl}$, and *Cd39*$^{fl/fl}$ control mice were exposed to 3,5-diethoxycarbonyl-1,4-dihydrocollidine (DDC) to induce biliary fibrosis. Hepatic hydroxyproline levels, liver histology, immunohistochemistry, mRNA expression levels, and serum biochemistry were then assessed. Following 3 weeks of DDC-feeding, *Cd39*$^{-/-}$ mice exhibited more severe fibrosis, when compared to WT mice as reflected by morphology and increased liver collagen content. Myeloid-specific CD39 deletion in LysMCre*Cd39*$^{fl/fl}$ mice recapitulated the phenotype of global *Cd39*$^{-/-}$, after exposure to DDC, and resulted in similar worsening of liver fibrosis when compared to *Cd39*$^{fl/fl}$ control animals. Further, DDC-treated LysMCre*Cd39*$^{fl/fl}$ mice exhibited elevated serum levels of transaminases and total bilirubin, as well as increased hepatic expression of the profibrogenic genes *Tgf-β1*, *Tnf-α*, and *α-Sma*. However, no clear differences were observed in the expression of macrophage-elaborated specific cytokines between LysMCre*Cd39*$^{fl/fl}$ and *Cd39*$^{fl/fl}$ animals subjected to biliary injury. Our results in the DDC-induced biliary type liver fibrosis model suggest that loss of CD39 expression on myeloid cells largely accounts for the exacerbated sclerosing cholangitis in global CD39 knockouts. These findings indicate that macrophage expressed CD39 protects from biliary liver injury and fibrosis and support a potential therapeutic target for human hepatobiliary diseases.

Keywords CD39 · Liver fibrosis · Primary sclerosing cholangitis · Kupffer cells · Purinergic signaling

Yury V. Popov and Simon C. Robson contributed equally to this work.

Electronic supplementary material The online version of this article (https://doi.org/10.1007/s11302-019-09664-3) contains supplementary material, which is available to authorized users.

✉ Yury V. Popov
ypopov@bidmc.harvard.edu

✉ Simon C. Robson
srobson@bidmc.harvard.edu

[1] Division of Gastroenterology and Hepatology, Beth Israel Deaconess Medical Center and Harvard Medical School, 330 Brookline Avenue, Dana 501, Boston, MA 02115, USA

[2] Department of Surgery, Charité Universitätsmedizin, Freie Universität Berlin, Humboldt-Universität zu Berlin and Berlin Institute of Health, 13353 Berlin, Germany

Abbreviations

ALP	alkaline phosphatase
ALT	alanine aminotransferase
α-Sma	α-smooth muscle actin
Col1a1	Collagen type 1 alpha 1
DDC	3,5-diethoxycarbonyl-1,4-dihydrocollidine
ECM	extracellular matrix
HSCs	hepatic stellate cells
KO	knockout
Mdr2	multidrug resistance protein 2
PSC	primary sclerosing cholangitis
qRT-PCR	real-time quantitative polymerase chain reaction
TBIL	total bilirubin
Tgf-β	transforming growth factor β
Tnf-α	tumor necrosis factor α
WT	wild-type

Introduction

Liver fibrosis, a wound-healing process, occurs in response to persistent liver cell damage irrespective of its cause. The net result of this process is the accumulation of extracellular matrix (ECM) proteins steadily replacing normal hepatic parenchyma with scar tissue. Any kind of ongoing liver injury induces various molecular and cellular changes including parenchymal cell proliferation, release of inflammatory signals, and immune cell infiltration, which all eventually result in deposition of ECM. Depending on the source of liver injury the fibrous pattern can differ, e.g., alcohol-induced liver disease shows perisinusoidal and pericentral fibrosis, while cholestatic conditions manifest with interstitial periportal ("biliary-type") fibrosis [1].

In cholangiopathies, like primary biliary cirrhosis and primary sclerosing cholangitis, the underlying cause of fibrosis is biliary injury. Over time, biliary fibrosis can progress to biliary cirrhosis and subsequently to end-stage liver disease making cholestatic liver diseases, despite its low prevalence, frequent indications for liver transplantation [2]. Although many pathophysiological features are shared with hepatic fibrosis, the mechanisms leading to biliary fibrosis during chronic cholestasis are partly different and are still poorly understood [3]. Cholestasis-induced fibrosis involves highly concerted interactions between activated reactive cholangiocytes, extracellular matrix-producing cells like portal myofibroblasts and hepatic stellate cells (HSCs), as well as inflammatory cells such as neutrophils, lymphocytes, and macrophages [3, 4].

The current view suggests that the ductular reaction, as a consequence to bile duct damage, initiates the fibrogenic cascade with reactive cholangiocytes producing cytokines, chemokines, growth factors, and profibrogenic factors [4, 5]. These factors in turn activate HSC and myofibroblasts to promote matrix production [6]. Further, the released proinflammatory mediators are associated with immune cell infiltration into the portal area further enhancing bile duct damage and also perpetuating biliary fibrosis [4].

Macrophages are involved in tissue injury and repair, including the pathogenesis of fibrosis [7]. These cells play a critical role in liver homeostasis, in reparative responses with subsequent inflammation and fibrogenesis, and moreover, they can promote fibrosis resolution [1, 8–10]. Accordingly, macrophages can exert various immunological functions and polarize into different phenotypes depending on the microenvironmental stimuli [8]. Based on phenotype and proposed functions, macrophages may be distinguished as classically activated macrophages, also referred to as M1 (pro-inflammatory), or as alternatively activated macrophages, also known as M2 (anti-inflammatory). This classification has some uses conceptually, but does not take into consideration intermediate activation states [9, 10]. To better understand the role of macrophages in the course of chronic liver injury and fibrosis, attempts have been made to characterize these putative macrophage phenotypes at different stages of tissue injury and repair. During fibrosis, the presence of the M1 phenotype seems to be predominate at the onset of injury [10, 11], whereas M2 macrophage deviation evolves when the acute phase of inflammation resolves [12]. Selective depletion of macrophages during the onset of liver injury prevents stellate cell activation and ameliorates fibrosis progression, whereas depletion of macrophages during the recovery phase attenuates matrix degradation and delays resolution [13–15]. The molecular mechanisms that regulate such transitions from M1 to M2 or from fibrogenic to fibrolytic macrophages all remain poorly defined.

Extracellular ATP functions as a "danger signal" that can modulate immune cell differentiation via P2 receptor activation [16]. CD39 hydrolyzes extracellular ATP/ADP to AMP, to be further metabolized to adenosine. This ATP metabolic pathway, balancing ATP and adenosine levels, has emerged as a potent regulator of immune cells, also modulating macrophage polarization [17, 18]. It has been shown that ATP favors pro-inflammatory M1 macrophages, whereas adenosine signaling induces the putatively anti-inflammatory M2 macrophages [19]. However, it remains unknown whether in the hepatic fibrotic response macrophage-expressed CD39 can tip the balance in favor of the adenosinergic, profibrogenic macrophage phenotype.

We have previously demonstrated that global CD39 deficiency worsens liver injury and fibrosis in the *Mdr2*$^{-/-}$ mouse model of sclerosing cholangitis. However, since CD39 is expressed on a wide variety of immune cells as well as endothelial cells, no conclusions could be drawn as to which CD39-expressing cell subset is instrumental in regulating biliary injury and fibrogenesis. In order to assess the role of CD39 in macrophages in the setting of biliary fibrosis, we generated macrophage CD39 null mice (LysMCre*Cd39*$^{fl/fl}$) by crossing CD39 floxed (*Cd39*$^{fl/fl}$) mice with LysMCre mice [20].

In this study, we aimed to elucidate the contribution of macrophage expressed CD39 to the inflammatory conditions, injury, and fibrosis in the experimental sclerosing cholangitis model induced by feeding of exogenous 3,5-diethoxycarbonyl-1,4-dihydrocollidine (DDC) to mice. Both mutant mice—with global and with myeloid-specific depletion of CD39—exhibited more pronounced biliary fibrosis, when compared to the respective control animals. Overall, our data suggests that selective CD39 expression on macrophages is a key regulator in the pathogenesis of cholestatic liver injury in this experimental model.

Material and methods

Animals

All experimental mice were kept in a pathogen-free, temperature-controlled room with alternating 12 h dark/light cycles. Water

and chow diet was provided ad libitum unless otherwise stated. All animal procedures were approved by the Institutional Animal Care and Use Committee at Beth Israel Deaconess Medical Center, Harvard Medical School (Boston, MA) (protocols 065-2015).

Cd39$^{-/-}$ and *Mdr2*$^{-/-}$ mice on the C57Bl/6 background were generated as previously described [21, 22]. In all experiments with *Cd39*$^{-/-}$ and *Mdr2*$^{-/-}$ mice, C57Bl/6 mice served as controls.

Generation of LysMCre*Cd39*$^{fl/fl}$ mice

Floxed *Cd39* mice were generated in collaboration with GenOway by inserting loxP sites in the *Cd39* gene locus allowing Cre-mediated excision of exons 5 to 6 containing the enzymatically active region. Deletion of exons 5 to 6 results in a frame-shift leading to a premature stop codon in exon 7. *Cd39*$^{fl/fl}$ mice were generated on a C57BL/6 genetic background. Homozygous *Cd39* floxed mice were crossed to *Lyz2tm1(cre)Ifo* (referred to as LysMCre) mice purchased from the Jackson Laboratory (both on C57Bl6 background) to generate macrophage-specific *Cd39* knockout mice (LysMCre*Cd39*$^{fl/fl}$). At weaning, mice were genotyped for LysMCre using a mix of mutant, wildtype, and common primers (mutant: 5′-CCC AGA AAT GCC AGA TTA CG-3′; wild-type: 5′-CTT GGG CTG CCA GAA TTT CTC-3′; common: 5′-TTA CAG TCG GCC AGG CTG AC-3′). Hetero-/homozygosity for floxed *Cd39* was assessed using forward and reverse primers detecting *Cd39* floxed alleles (5′-TTAGTGAGGCTGAGGCAGGAGAGTTGC-3′ and 5′-CCAGCAAGAGGGCTTTGAAGACACAG-3′). In all experiments with LysMCre*Cd39*$^{fl/fl}$ mice, *Cd39*$^{fl/fl}$ littermates served as controls.

DDC (3,5-diethoxycarbonyl-1,4-dihydrocollidine) -induced model of biliary fibrosis

DDC feeding induces bile duct injury, cholangitis, ductular reaction, and portal-portal bridging fibrosis [3], recapitulating clinical features of human biliary fibrosis. Mice at the age of 8 weeks were fed a control diet or a DCC-supplemented diet (0.1%) for 3 weeks to induce advanced biliary fibrosis as described [23]. The differences between DDC-fed mice and healthy control animals (receiving control diet) were calculated for each group. The alterations in values between WT or *Cd39*$^{fl/fl}$ and CD39 deficient animals were contrasted, by using the WT/*Cd39*$^{fl/fl}$ delta as reference.

Immunohistochemistry and immunofluorescence were performed as previously reported (24, 25). Primary antibodies were F4/80 (#MCA497; Bio-Rad, Hercules, CA, USA) and CD39 for IF (C9F, kind gift from Jean Sévigny, Centre de Recherche du CHU de Québec, Université Laval, Quebec, Canada), as well as CD39 (#AF-4398; R&D Systems, Minneapolis, MN, USA) and pan-Cytokeratin for IHC (#Z0622; Dako, Agilent Technologies, Santa Clara, CA, USA). In DDC-fed mice, staining was developed using ImmPACT VIP Peroxidase (#SK-4605, Vector Laboratories, Burlingame, CA), which results in a purple reaction product distinct from the brownish porphyrine plugs present in DDC-fed livers. In all other animals, ImmPACT DAB Peroxidase (#SK-4100, Vector Laboratories) for brown color development was used. All slides were examined and recorded on a Nikon microscope. Immunofluorescence was performed on acetone-fixed frozen liver sections with DAPI as a nuclear counterstain. Images were captured using Zeiss Axioimager M1 (Carl Zeiss, Oberkochen, Germany).

Hepatic collagen was quantified using a biochemical assay that measures the hydroxyproline content. The assay was performed using two liver sections from the median and left lobe (250–300 mg in total, representing at least 10% of total liver volume), as previously described [24]. Hepatic collagen content was expressed as relative hepatic hydroxyproline levels (per 100 mg of wet liver).

Serum levels of alanine aminotransferase (ALT), alkaline phosphatase (ALP), and total bilirubin (TBIL) were measured on automated Catalyst Dx Chemistry Analyzer (IDEXX Laboratories, Inc., Westbrook, ME) according to the manufacturer's instructions.

Peritoneal macrophages were harvested from the peritoneal cavity of adult *Cd39*$^{fl/fl}$, *Cd39*$^{-/-}$, or LysMCre*Cd39*$^{fl/fl}$ mice by lavaging the cavity with cold PBS. Peritoneal cells were washed and thereafter analyzed by flow cytometry.

Flow cytometry Peritoneal macrophages or splenocytes were stained with PB CD11b (clone M1/70, #101223), FITC CD19 (clone 6D5, #115506), APC CD45R/B220 (clone RA3-6B2, #103211) (BioLegend, San Diego, CA) FITC F4/80 (clone BM8, #11-4801-82), PE CD39 (clone 24DMS1, #12-0391-82) (Thermo Fisher, Burlingame, CA). Cells were incubated at 4 °C in the dark for 30 min and washed with phosphate-buffered saline, supplemented with 1% fetal calf serum, before analysis was made. For surface marker analysis, macrophages were gated based on the F4/80 + CD11b + population, whereas splenic B-cells were identified based on CD19 and B220 (CD45R) expression. Samples were analyzed using GalliosTM flow cytometer (Beckman Coulter, Brea, CA) and Kaluza software (Beckman Coulter).

RNA isolation and real-time quantitative polymerase chain reaction At harvest, liver tissue was snap frozen in liquid nitrogen and stored at − 80 °C until further processing. Total RNA was isolated from frozen liver tissue using TRIzol® reagent (Life Technologies, Carlsbad, CA) according to the manufacturer's protocol. Reverse transcription of total RNA was done using the iScriptTM cDNA Synthesis kit (Bio-Rad, Hercules, CA). Real-time quantitative polymerase chain

reaction (qRT-PCR) was performed on a Stratagene Mx3005P (Agilent Technologies, Santa Clara, CA) with the TaqMan and SYBR Green methodology. Sequences of primers and probes are summarized in Supplementary Table 1.

Statistical analysis Data are expressed as mean ± standard error of mean and were analyzed using Graph-Pad Prism version 5.0 (GraphPad Software, San Diego, CA). Statistical comparisons between two groups were performed by the Student's *t* test. *P* values < 0.05 were considered significant.

Results

Hepatic biliary fibrosis induced by DDC is more pronounced in *Cd39*$^{-/-}$ mice

To assess the effect of global CD39 loss on DDC-induced cholestatic liver injury, CD39 null mice (*Cd39*$^{-/-}$) and WT control mice were treated with a DDC-containing diet for 3 weeks. Histopathological analysis of DDC-fed mouse livers showed a pronounced ductular reaction with periportal fibrosis. *Cd39*$^{-/-}$ mice had more pronounced fibrotic responses than that noted in control animals, as indicated by Sirius Red staining (Fig. 1a). Biochemical quantification of liver collagen content via hydroxyproline determination confirmed this histological observation, with close to 30% increases in collagen accumulation in CD39 null mice, as compared to WT animals ($p = 0.0233$) (Fig. 1b). Consistently, upregulated mRNA expression of *Col1a1* and *α-Sma* confirmed the increased DDC-induced collagen deposition in *Cd39*$^{-/-}$ mice compared to WT mice (Suppl. Fig. 1).

This increased fibrotic response was unexpectedly not associated with significant increases in liver injury and function markers at 3 weeks study end-point, as assessed by serum levels of ALT, ALP, and total bilirubin, which were comparable between *Cd39*$^{-/-}$ and WT mice after DDC feeding (Fig. 1c). Next, we aimed to further investigate the role of CD39 and macrophages in the *Mdr2*$^{-/-}$ and DDC-induced models of sclerosing cholangitis. Compared to control animals, increased numbers of F4/80-positive macrophages and CD39-positive cells were found in both injury models. Immunohistochemical staining for CD39 and F4/80 revealed an accumulation of macrophages and CD39^{+} cells predominantly in the portal areas, suggesting involvement of these cells in biliary fibrosis (Fig. 1d).

Generation of myeloid specific CD39 knockout mice

To examine the role of macrophage CD39 in the development of biliary fibrosis, we generated mice selectively lacking CD39 expression in macrophages. Mice with a floxed *Cd39* allele with loxP sites flanking exon 5 and 6 were crossed with mice harboring the Cre recombinase under the *LysM* promoter (Fig. 2a), which is expressed in neutrophils and macrophages [25]. The homologous recombination mediated by the Cre/loxP system deletes exon 5 and 6, which encode, at least in part, the CD39 enzymatically active region [26]. These events result in CD39 deficiency in cells of myeloid lineage. Genomic expression of the floxed *Cd39* allele and LysMCre was assessed by PCR using primers specific for Cre and the mutant CD39. Mating of *Cd39*$^{fl/fl}$ with LysMCre mice resulted in LysMCre*Cd39*$^{fl/fl}$ mice, as confirmed by the genotype results confirming the presence of the floxed *Cd39* allele and the LysMCre transgene (Fig. 2b).

CD39 deletion efficiency on peritoneal macrophages from LysMCre*Cd39*$^{fl/fl}$ mice was assessed by flow cytometry (Fig. 2c), which revealed that only approximately 13% of macrophages retained CD39 expression. In contrast, peritoneal macrophages from *Cd39*$^{-/-}$ mice, serving as a positive control, displayed less than 1% CD39 positivity. Flow cytometry analysis in peritoneal macrophages from *Cd39*$^{fl/fl}$ mice, used as control animals in this study, revealed CD39 expression in 100% of the cells, as expected.

The specificity of LysMCre-mediated gene deletion was tested by flow cytometry of B cells isolated from the spleen (Fig. 2d). B cells from LysMCre*Cd39*$^{fl/fl}$ mice expressed CD39 in about 64% of the cells, which was comparable with *CD39*$^{fl/fl}$ splenocytes, expressing CD39 in 86% of all B cells. Again, CD39 expression was less than 1% in *Cd39*$^{-/-}$ B cells.

To demonstrate absence of CD39 in Kupffer cells—the resident liver macrophages—double immunofluorescent in situ staining of CD39 and F4/80 was performed on liver sections (Fig. 2e). In livers from *Cd39*$^{fl/fl}$ mice, most F4/80^{+} cells were also CD39^{+}. In contrast, Kupffer cells (detected by F4/80) from LysMCre*Cd39*$^{fl/fl}$ livers showed no CD39 positivity. CD39 staining was still present in endothelial cells, indicating that in LysMCre*Cd39*$^{fl/fl}$ mice, CD39 is specifically deleted in Kupffer cells and hepatic myeloid cells (Fig. 2e).

CD39 depletion in macrophages exacerbates DDC-induced biliary fibrosis and liver injury

To evaluate the contribution of macrophage-specific CD39 to liver inflammation and fibrosis, LysMCre*Cd39*$^{fl/fl}$ mice and *Cd39*$^{fl/fl}$ controls were fed a DDC containing diet for 3 weeks. Sirius Red staining of livers from DDC-fed mice revealed increased fibrosis in LysMCre*Cd39*$^{fl/fl}$ animals compared to controls, as reflected by denser deposition of collagen around proliferating bile ducts (note the more intense red staining in LysMCre*Cd39*$^{fl/fl}$ mice) (Fig. 3a). Hepatic collagen content was significantly increased in DDC-fed LysMCre*Cd39*$^{fl/fl}$ mice, which was accompanied by a 107.7% higher increase in hepatic collagen content (hydroxyproline) in DDC-fed LysMCre*Cd39*$^{fl/fl}$ mice versus DDC-treated *Cd39*$^{fl/fl}$ mice in comparison to healthy controls ($p < 0.0001$, Fig. 3b). DDC

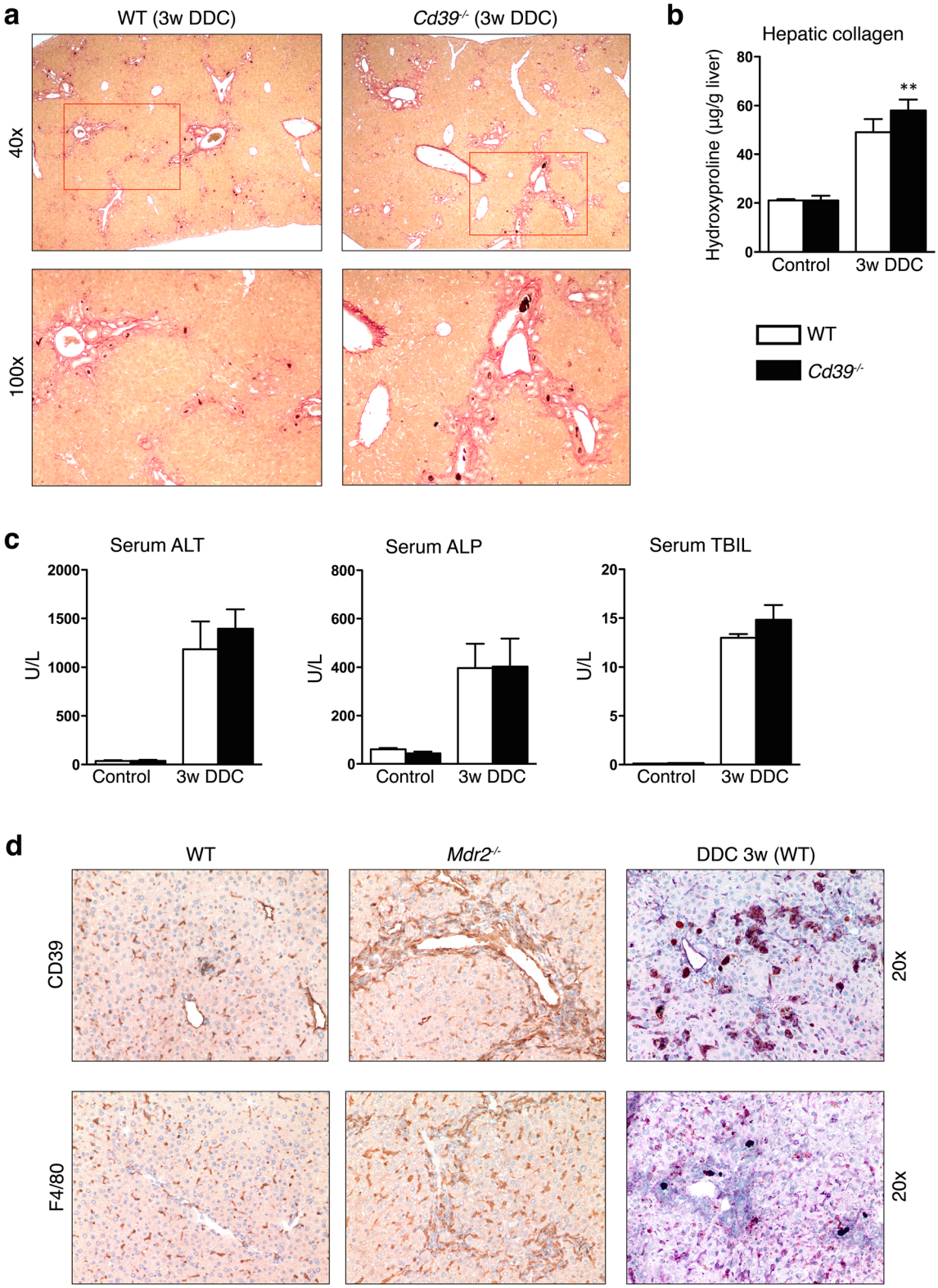

Fig. 1 CD39 deficiency worsens liver fibrosis in the DDC-induced model of biliary fibrosis. **a** Representative images of Sirius Red stained liver sections from WT and CD39 KO mice after 3 weeks of DDC feeding (original magnification × 40 in the upper and × 100 in the lower panel). **b**, **c** Relative hepatic collagen content (µg/g liver), serum ALT, ALP, and TBIL in age-matched WT and CD39 null mice after 3 weeks DDC administration or standard chow diet. Data are shown as mean ± SEM ($n = 5–8$ animals per bar). $^{**}P \leq 0{,}001$. **d** Liver sections from WT, *Mdr2*$^{-/-}$, and DDC-fed WT mice were subjected to immunohistochemistry for CD39 (upper panel) and F4/80 (lower panel) (original magnification × 20)

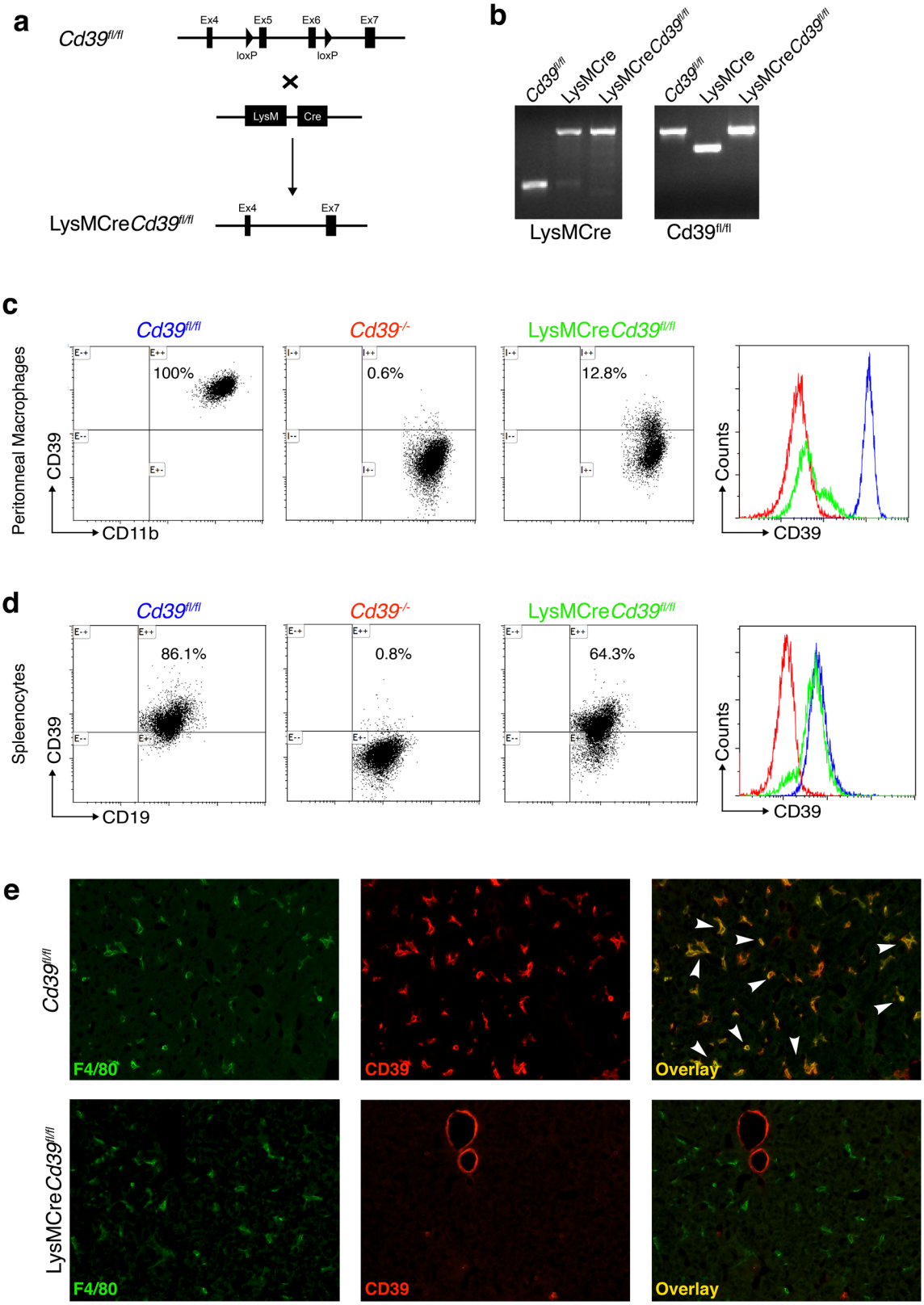

feeding was also associated with liver injury in LysMCre*Cd39*$^{fl/fl}$ mice as evidenced by increased ALT (1424 ± 69.83 vs. 1115 ± 87.27 U/L, $p = 0.0167$), ALP (378 ± 25.27 vs 229 ± 18.48, $p < 0.0001$), and TBIL (11.5 ± 1.019 vs. 5.14 ± 0.7959, $p < 0.0001$) serum levels (Fig. 3c). Because macrophages express CD39 (Fig. 2e), we asked whether loss

◀ **Fig. 2** Generation and characterization of macrophage specific CD39 KO mice (LysMCre*Cd39*$^{fl/fl}$). **a** Schematic illustration of gene deletion strategy. Mice carrying the *Cd39* gene construct with 2 loxP sites flanking exon 5 and 6 were crossed with LysMCre mice to generate LysMCre*Cd39*$^{fl/fl}$ mice. **b** LysMCre*Cd39*$^{fl/fl}$ mice show expression of both, LysMCre and CD39 floxed fragments, monitored by polymerase chain reaction. **c** Flow cytometry analysis of peritoneal macrophages (F4/80^{+}CD11b^{+}) confirms effective Cre-mediated CD39 deletion in LysMCre*Cd39*$^{fl/fl}$ mice. *Cd39*$^{fl/fl}$ and *Cd39*$^{-/-}$ mice were included as positive and negative controls. Histogram shows CD39 expression in gated macrophages. Blue: *Cd39*$^{fl/fl}$, red: *Cd39*$^{-/-}$, green: LysMCre*Cd39*$^{fl/fl}$. **d** Flow cytometry analysis of splenocytes from LysMCre*Cd39*$^{fl/fl}$ mice shows CD39 expression in splenic B cells (B220^{+}CD19^{+}) from *Cd39*$^{fl/fl}$ (positive control) and *Cd39*$^{-/-}$ (negative control) mice. Representative histogram showing expression of CD39 in B cells of *Cd39*$^{fl/fl}$ (blue), *Cd39*$^{-/-}$ (red), and LysMCre*Cd39*$^{fl/fl}$ (green) mice. **e** Immunofluorescence staining for F4/80 (green) and CD39 (red) in frozen liver sections shows specific CD39 deletion in Kupffer cells from LysMCre*Cd39*$^{fl/fl}$ mice, but not in endothelial cells. Kupffer cells and endothelial cells in *Cd39*$^{fl/fl}$ livers show CD39 expression (original magnification, × 200)

of CD39 in these cells affects macrophage numbers in the liver. Therefore, we examined the gene expression of the macrophage marker *Cd68* and performed immunohistochemical analysis using the macrophage marker F4/80. In control LysMCre*Cd39*$^{fl/fl}$ mice and *Cd39*$^{fl/fl}$ mice, the hepatic mRNA levels of *Cd68* were comparable (Suppl. Fig. 2a). Moreover, the pattern and extent of macrophage infiltration in DDC-fed LysMCre*Cd39*$^{fl/fl}$ and *Cd39*$^{fl/fl}$ mice was similar, indicating that macrophage numbers were not altered under normal conditions or during biliary injury (Suppl. Fig. 2b). To further assess the role of macrophage CD39 in DDC-induced biliary fibrosis, gene expression of the profibrogenic markers *Tgf-β1*, *Tnf-α*, and *α-Sma* was measured in the liver. The mRNA levels of *Tgf-β1*, *Tnf-α*, and *α-Sma* were significantly increased in LysMCreCd39$^{fl/fl}$ animals compared with control mice, whereas there was no change in the expression of *Col1a1* (Fig. 4a).

DDC supplementation caused a reactive phenotype of biliary epithelial cells, leading to ductular reaction and periductal fibrosis [3]. Since ductular reaction has been shown to correlate with fibrosis severity [27], we assessed whether ductular expansion was different between LysMCre*Cd39*$^{fl/fl}$ and control mice. However, DDC feeding resulted in a comparable extent of ductular reaction in both groups as indicated by morphometry of pan-cytokeratin-positive cells (Fig. 4b).

CD39 plays a major role in the termination of ATP signaling, which is involved in the regulation of numerous immune responses, including macrophage polarization [19]. Therefore, we aimed to explore if in the sclerosing cholangitis model, CD39-deficient macrophages are polarized towards a pro-inflammatory phenotype. Quantitative RT-PCR of whole

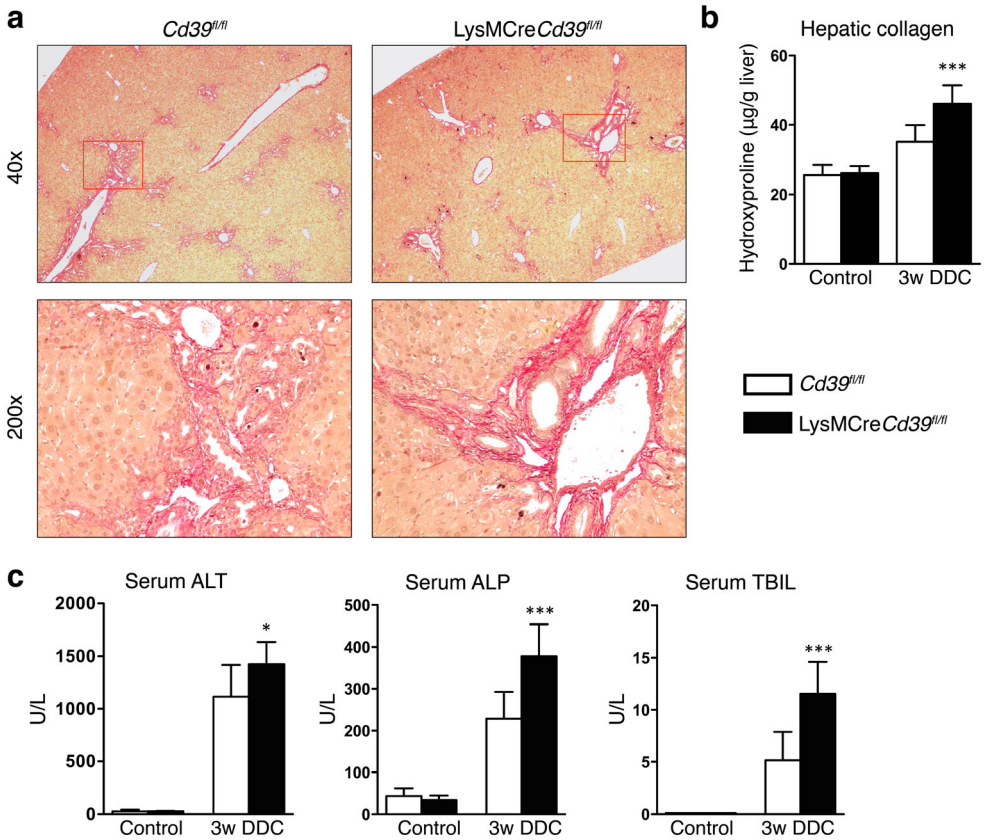

Fig. 3 Loss of CD39 on macrophages increases biliary fibrosis and liver injury in the DDC-fed liver fibrosis model. **a** Representative images of Sirius Red stained liver sections from *Cd39*$^{fl/fl}$ and LysMCre*Cd39*$^{fl/fl}$ mice after 3 weeks of DDC feeding (original magnification × 40 in the upper panel and ×200 in the lower panel). **b**, **c** Relative hepatic collagen content (µg/g liver), serum ALT, ALP, and TBIL in age-matched WT and CD39 null mice after 3 weeks DDC administration or standard chow diet. Data are shown as mean ± SEM ($n = 5$–8 animals per bar). *$P \leq 0.05$, ***$P \leq 0.001$

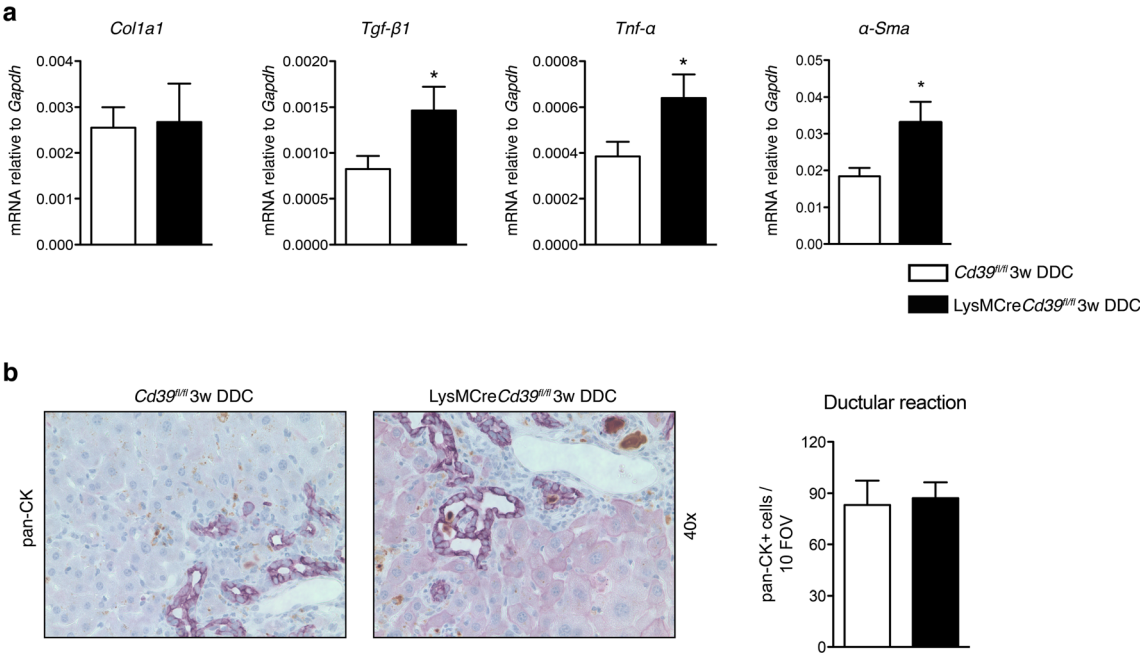

Fig. 4 Loss of CD39 on macrophages increases biliary fibrosis and causes more liver injury in the DDC-fed liver fibrosis model. **a** qRT-PCR was performed to test the expression of the pro-fibrogenic genes *Tgf-β1*, *Tnf-α*, *α-Sma*, and *Col1a1* in whole liver tissue. **b** Representative pan-cytokeratin (p-CK) immunohistochemistry of liver sections from DDC fed $Cd39^{fl/fl}$ and LysMCre$Cd39^{fl/fl}$ mice and quantification of pan-CK staining (10 random portal fields, $n = 3$, × 40). Statistical significance was assessed using unpaired *t*-test with $^{*}P \leq 0.05$

livers showed similar expression levels of the M1 associated pro-inflammatory cytokines (*Ifng*, *Il1b*, and *Il6*) as well as of the M2 associated immunosuppressive cytokine, *Il10* (Fig. 5). However, no differences were detected in the expression of these cytokine markers, *iNos* or *Arg1* (Fig. 5). In vitro analysis of bone-marrow derived macrophages after LPS stimulation also indicated no substantive differences for *Il1b*, *Il6*, or *Tnf-α* (data not shown).

Collectively, these results suggest that loss of CD39 on macrophages is associated with more pronounced biliary

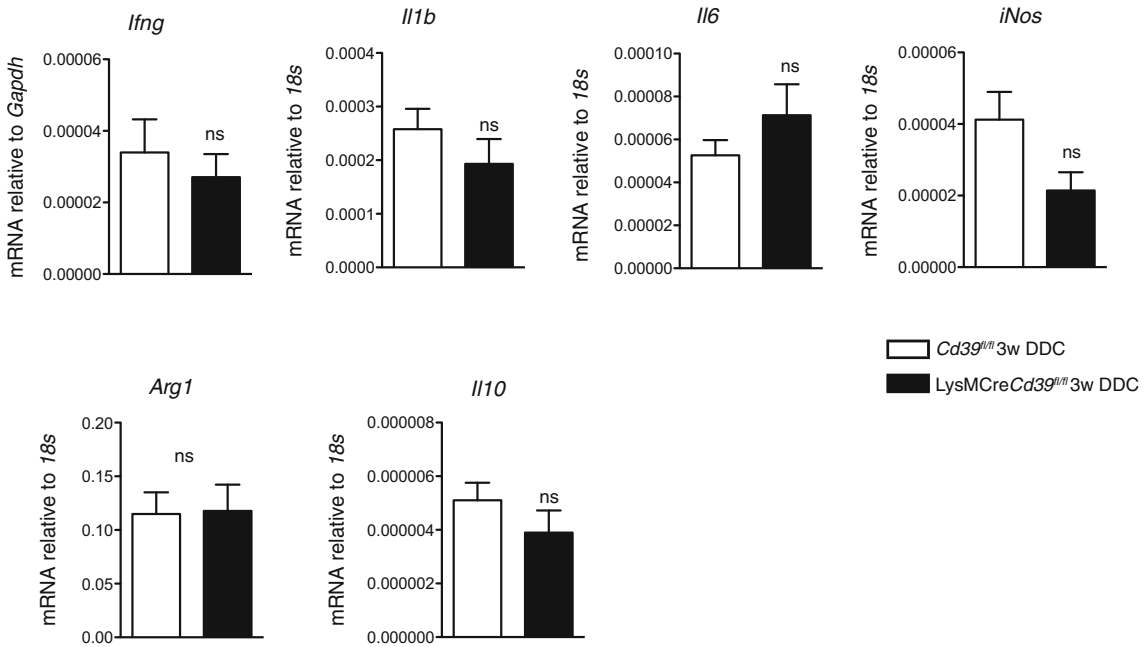

Fig. 5 Profile expression patterns of macrophage cytokines are comparable in livers of LysMCre$Cd39^{fl/fl}$ and control mice. Expression of *Ifng*, *Il1b*, *Il6*, *iNos*, *Arg1*, and *Il10* mRNA levels was measured in DDC-fed LysMCre$Cd39^{fl/fl}$ and $Cd39^{fl/fl}$ mice by qRT-PCR. Values are presented as mean ± SEM. ns, not significant (*t* test)

injury and fibrosis, which appear to be mediated by an intermediate, non-canonical macrophage phenotype.

Discussion

We have previously reported that global loss of CD39 exacerbates liver injury and fibrosis in the human primary sclerosing cholangitis (PSC)-like *Mdr2*$^{-/-}$ mouse model [22]. We now show that global CD39 deletion worsens biliary fibrosis induced by DDC feeding, as another experimental model of PSC. In this present study, we also report, for the first time, mice deficient for CD39 in myeloid cells, which were generated using the Cre-loxP system. Using these cell-specific, CD39 targeted deletions, we provide supportive evidence that macrophage CD39 contributes substantially to the CD39 global null phenotype in the setting of biliary injury and fibrosis. The increase in the content of hepatic collagen in these settings is accompanied by elevated liver tests as well as by increased expression of the pro-fibrogenic gene *Tgf-β1* and the proinflammatory gene *Tnf-α*.

DDC-fed CD39 null mice show worsening of biliary fibrosis compared to DDC-fed WT mice, implicating the involvement of the ectonucleotidase during liver fibrosis. However, CD39 is expressed by both, macrophages and sinusoidal cells (Fig. 2) [28, 29]. We hypothesized that macrophage CD39 is functionally important for two reasons: this ectoenzyme plays a key role in controlling the activation and the phenotype of macrophages [30]; and that further macrophages are central in the development and resolution of liver fibrosis [26–28, 31, 32].

The pivotal role of macrophages during liver fibrogenesis is also reflected by several studies investigating the modulation of macrophage functions as an anti-fibrotic therapeutical strategy [33, 34]. The CCR2/CCR5 antagonist cenicriviroc has been evaluated in an open-label proof-of-concept trial in patients with PSC (PERSEUS, NCT02653625), with the results still awaiting publication. In another phase 2b clinical trial, safety and efficacy of cenicriviroc, have been assessed in 289 patients with NASH and fibrosis for the treatment of non-alcoholic steatohepatitis with liver fibrosis (CENTAUR, NCT02217475) [35]. Patients treated with Cenicriviroc for 1 year were twice as likely to have less fibrosis when compared to the placebo group; safety and tolerability were comparable to placebo [36]. For further confirmation, the AURORA phase 3 trial is underway (AURORA, NCT03028740).

In different experimental in vivo models, the pharmacological inhibition of CCR2-dependent monocyte/macrophage recruitment during biliary injury resulted in significantly lower collagen deposition and decreased plasma ALT and AST [35, 37]. Given the dualistic role of macrophages in liver fibrosis, therapeutic strategies that enhance immunosuppressive features of these cells might represent an additional antifibrotic approach, which are currently under investigation in several experimental and clinical studies [38]. Further, modulation of macrophage polarization using nanomedicine has been investigated as a novel therapeutic modality to inhibit or reverse fibrosis. The attempt to deliver dexamethasone via liposomes to macrophages was effective; however, besides Kupffer cells also inflammatory macrophages and T cells showed liposome accumulation. Dexamethason-loaded liposomes reduced the numbers of hepatic inflammatory macrophages and promoted the anti-inflammatory M2 macrophage phenotype, but also significantly reduced the numbers of T-cells in the liver. In the carbon tetrachloride (CCl4)-based model of chronic liver injury, liposomal dexamethasone has shown some antifbrotic efficacy. Nevertheless, nanoparticle based approaches need further refinement prior to use in the clinical setting [39]. In line with these studies, we observed hepatic macrophage accumulation in the DDC mouse model using CD39 global null and macrophage-specific CD39 KO mice. Even though lack of macrophage CD39 did not cause differences in the number of infiltrating macrophages, increased liver injury and upregulation of the *Tgf-β1* and *Tnf-α* transcripts was demonstrated. Thus, we speculate that CD39 is involved in regulating the macrophage phenotype in cholestatic conditions. However, we could not identify a clear M1 or M2 phenotype in our present study and further research is needed to better understand how CD39 signaling and macrophages contribute to the pathogenesis of sclerosing cholangitis.

Overall, the development of novel anti-fibrotic therapies requires a thorough understanding of the mechanisms that regulate the macrophage phenotype and functionality during the different stages of liver fibrosis. Although the signaling pathways regulating macrophage polarization remain incompletely understood, several reports indicated involvement of CD39 in controlling activation and transitional differentiation of these cells [19, 40].

Extracellular nucleotides are well-established regulators of various immune cell fates. [41] In recent years, a more detailed understanding of the role played by the purinergic signaling in macrophage differentiation has been achieved. ATP, released from inflamed tissue, recruits monocytes and through activation of the inflammasome induces polarization into proinflammatory macrophages [19]. On the other hand, adenosine prevents the classical macrophage activation and instead favors the anti-inflammatory phenotype characterized by increased IL-10 production, Arginase 1 expression, and lower levels of TNF-α and IL-12 secretion. [19] CD39, as the major ectonucleotidase hydrolyzing ATP into adenosine precursors, balances these two opposing responses [17].

Toll-like receptor mediated signaling stimulates macrophages to produce endogenous ATP. ATP is hydrolyzed to adenosine by CD39 expressed on macrophage membrane, which in turn induces a regulatory macrophage phenotype with attenuated inflammatory cytokine production and enhanced IL-10 expression. Hence, macrophages lacking

CD39 are unable to transition to the anti-inflammatory state and, instead, promote inflammation. Based on these findings, others and we have suggested that macrophage CD39 acts as a "molecular" switch enabling macrophages and other cells to transition from the inflammatory to the regulatory, anti-inflammatory phenotype.

In agreement with these findings, we have observed exacerbations in liver fibrosis in LysMCre*Cd39*$^{fl/fl}$ mice in the DDC diet model suggesting that CD39 deficient macrophages maintain the pro-inflammatory state, as evidenced by increased levels of *Tnf-α*. Despite the clear caveats, the gene expression data and in vitro analysis of macrophage differentiation after LPS stimulation did not indicate clear phenotypic signatures. It should, however, be noted that the M1/M2 classification does not account for all the various macrophage phenotypes, which might be acquired in a dynamic process as a response to environmental triggers. Furthermore, individual macrophages can express M1 and M2 phenotypic markers simultaneously [42], suggesting caution in the classification and compartmentalization of these responses.

In summary, we have now demonstrated in distinct models of PSC that CD39 protects from biliary injury and fibrosis. Our studies further indicate that macrophage expressed CD39 contributes to the CD39 null phenotype in biliary injury and fibrosis. More research is needed to better understand how purinergic signaling modulates macrophage activation and to fully define functional roles of alternative pathways of macrophage differentiation in the setting of hepatobiliary injury and fibrosis. Our studies provide hints that macrophage modulation could be a therapeutic opportunity in the management of hepatobiliary diseases.

Acknowledgements This study was supported by a research award from the Dept. of the Army USAMRAA (W81XWH-15-PRMRP-FPA; DoD) and a NIH grant (5R01DK108894-02) to S.C.R.

S.R. was a recipient of career development award from the Swiss National Science Foundation (P300PB_161098).

A research grant from PSC Partners Seeking a Cure Canada to Y.P. supported this work.

Funding This study was supported by a research award from the Dept. of the Army USAMRAA (W81XWH-15-PRMRP-FPA; DoD) and a NIH grant (5R01DK108894-02) to S.C.R.

Compliance with ethical standards

Ethical approval "All procedures performed in studies involving animals were in accordance with the ethical standards of the institution or practice at which the studies were conducted."

S.R. was a recipient of career development award from the Swiss National Science Foundation (P300PB_161098).

A research grant from PSC Partners Seeking a Cure Canada to Y.P. supported this work.

Conflict of interest The authors declare that they have no conflict of interest.

References

1. Bataller R, Brenner DA (2005) Liver fibrosis. J Clin Invest 115: 209–218. https://doi.org/10.1172/JCI24282
2. O'Leary JG, Lepe R, Davis GL (2008) Indications for liver transplantation. Gastroenterology 134:1764–1776. https://doi.org/10.1053/j.gastro.2008.02.028
3. Fickert P, Stöger U, Fuchsbichler A, Moustafa T, Marschall HU, Weiglein AH, Tsybrovskyy O, Jaeschke H, Zatloukal K, Denk H, Trauner M (2007) A new xenobiotic-induced mouse model of Sclerosing cholangitis and biliary fibrosis. Am J Pathol 171:525–536. https://doi.org/10.2353/ajpath.2007.061133
4. Lazaridis KN, Strazzabosco M, LaRusso NF (2004) The cholangiopathies: disorders of biliary epithelia. Gastroenterology 127:1565–1577. https://doi.org/10.1053/j.gastro.2004.08.006
5. Glaser SS, Gaudio E, Miller T, Alvaro D, Alpini G (2009) Cholangiocyte proliferation and liver fibrosis. Expert Rev Mol Med 11:e7. https://doi.org/10.1017/S1462399409000994
6. Popov Y, Schuppan D (2009) Targeting liver fibrosis: strategies for development and validation of antifibrotic therapies. Hepatology 50:1294–1306. https://doi.org/10.1002/hep.23123
7. Murray PJ, Wynn TA (2011) Protective and pathogenic functions of macrophage subsets. Nat Rev Immunol 11:723–737. https://doi.org/10.1038/nri3073
8. Gordon S, Martinez FO (2010) Alternative activation of macrophages: mechanism and functions. Immunity 32:593–604. https://doi.org/10.1016/j.immuni.2010.05.007
9. Martinez FO, Sica A, Mantovani A, Locati M (2008) Macrophage activation and polarization. Front Biosci 13:453–461 https://doi.org/10.2741/2692
10. Tacke F, Zimmermann HW (2014) Macrophage heterogeneity in liver injury and fibrosis. J Hepatol 60:1090–1096. https://doi.org/10.1016/j.jhep.2013.12.025
11. Wynn TA, Barron L (2010) Macrophages: master regulators of inflammation and fibrosis. Semin Liver Dis 30:245–257. https://doi.org/10.1055/s-0030-1255354
12. Braga TT, Agudelo JSH, Camara NOS (2015) Macrophages during the fibrotic process: M2 as friend and foe. Front Immunol 6. https://doi.org/10.3389/fimmu.2015.00602
13. Rivera CA, Bradford BU, Hunt KJ, Adachi Y, Schrum LW, Koop DR, Burchardt ER, Rippe RA, Thurman RG (2001 Jul) (2001) attenuation of CCl4-induced hepatic fibrosis by GdCl3 treatment or dietary glycine. Am J Physiol Gastrointest Liver Physiol 281(1): G200–G207. https://doi.org/10.1152/ajpgi.2001.281.1.G200
14. Duffield JS, Forbes SJ, Constandinou CM, Clay S, Partolina M, Vuthoori S, Wu S, Lang R, Iredale JP (2005) Selective depletion of macrophages reveals distinct, opposing roles during liver injury and repair. J Clin Investig 115:56–65. https://doi.org/10.1172/JCI22675
15. Best J, Verhulst S, Syn W-K, Lagaisse K, van Hul N, Heindryckx F, Sowa JP, Peeters L, van Vlierberghe H, Leclercq IA, Canbay A, Dollé L, van Grunsven LA (2016) Macrophage depletion attenuates extracellular matrix deposition and Ductular reaction in a mouse model of chronic Cholangiopathies. PLoS One 11:e0162286. https://doi.org/10.1371/journal.pone.0162286
16. Idzko M, Ferrari D, Eltzschig HK (2014) Nucleotide signalling during inflammation. Nature 509:310–317. https://doi.org/10.1038/nature13085
17. Cohen HB, Briggs KT, Marino JP, Ravid K, Robson SC, Mosser DM (2013) TLR stimulation initiates a CD39-based autoregulatory mechanism that limits macrophage inflammatory responses. Blood 122:1935–1945. https://doi.org/10.1182/blood-2013-04-496216
18. Haskó G, Cronstein B (2013) Regulation of inflammation by adenosine. Front Immunol 4(85). https://doi.org/10.3389/fimmu.2013.00085

19. Cekic C, Linden J (2016) Purinergic regulation of the immune system. Nat Rev Immunol 16:177–192. https://doi.org/10.1038/nri.2016.4
20. Clausen BE, Burkhardt C, Reith W, Renkawitz R, Förster I (1999) Conditional gene targeting in macrophages and granulocytes using LysMcre mice. Transgenic Res 8:265–277
21. Enjyoji K, Sévigny J, Lin Y, Frenette PS, Christie PD, Esch JSA, Imai M, Edelberg JM, Rayburn H, Lech M, Beeler DL, Csizmadia E, Wagner DD, Robson SC, Rosenberg RD (1999) Targeted disruption of cd39/ATP diphosphohydrolase results in disordered hemostasis and thromboregulation. Nat Med 5:1010–1017. https://doi.org/10.1038/12447
22. Peng Z, Rothweiler S, Wei G et al (2017) The ectonucleotidase ENTPD1/CD39 limits biliary injury and fibrosis in mouse models of sclerosing cholangitis. Hepatol Commun 1:957–972. https://doi.org/10.1002/hep4.1084
23. Peng Z-W, Ikenaga N, Liu SB, Sverdlov DY, Vaid KA, Dixit R, Weinreb PH, Violette S, Sheppard D, Schuppan D, Popov Y (2016) Integrin αvβ6 critically regulates hepatic progenitor cell function and promotes Ductular reaction, fibrosis, and tumorigenesis. Hepatology 63:217–232. https://doi.org/10.1002/hep.28274
24. Popov Y, Sverdlov DY, Sharma AK, Bhaskar KR, Li S, Freitag TL, Lee J, Dieterich W, Melino G, Schuppan D (2011) Tissue transglutaminase does not affect fibrotic matrix stability or regression of liver fibrosis in mice. Gastroenterology 140:1642–1652. https://doi.org/10.1053/j.gastro.2011.01.040
25. Jakubzick C, Bogunovic M, Bonito AJ, Kuan EL, Merad M, Randolph GJ (2008) Lymph-migrating, tissue-derived dendritic cells are minor constituents within steady-state lymph nodes. J Exp Med 205:2839–2850. https://doi.org/10.1084/jem.20081430
26. Pinsky DJ, Broekman MJ, Peschon JJ, Stocking KL, Fujita T, Ramasamy R, Connolly ES Jr, Huang J, Kiss S, Zhang Y, Choudhri TF, McTaggart RA, Liao H, Drosopoulos JHF, Price VL, Marcus AJ, Maliszewski CR (2002) Elucidation of the thromboregulatory role of CD39/ectoapyrase in the ischemic brain. J Clin Invest 109:1031–1040. https://doi.org/10.1172/JCI10649
27. Gouw ASH, Clouston AD, Theise ND (2011) Ductular reactions in human liver: diversity at the interface. Hepatology 54:1853–1863. https://doi.org/10.1002/hep.24613
28. Robson SC, Wu Y, Sun X, Knosalla C, Dwyer K, Enjyoji K (2005) Ectonucleotidases of CD39 family modulate vascular inflammation and thrombosis in transplantation. Semin Thromb Hemost 31:217–233. https://doi.org/10.1055/s-2005-869527
29. Bono MR, Fernández D, Flores-Santibáñez F et al (2015) CD73 and CD39 ectonucleotidases in T cell differentiation: beyond immunosuppression. FEBS Lett 589:3454–3460. https://doi.org/10.1016/j.febslet.2015.07.027
30. Lévesque SA, Kukulski F, Enjyoji K, Robson SC, Sévigny J (2010) NTPDase1 governs P2X7-dependent functions in murine macrophages. Eur J Immunol 40:1473–1485. https://doi.org/10.1002/eji.200939741
31. Pellicoro A, Ramachandran P, Iredale JP, Fallowfield JA (2014) Liver fibrosis and repair: immune regulation of wound healing in a solid organ. Nat Rev Immunol 14:181–194. https://doi.org/10.1038/nri3623
32. Pradere J-P, Kluwe J, De Minicis S et al (2013) Hepatic macrophages but not dendritic cells contribute to liver fibrosis by promoting the survival of activated hepatic stellate cells in mice. Hepatology 58:1461–1473. https://doi.org/10.1002/hep.26429
33. Thomas JA, Pope C, Wojtacha D, Robson AJ, Gordon-Walker TT, Hartland S, Ramachandran P, van Deemter M, Hume DA, Iredale JP, Forbes SJ (2011) Macrophage therapy for murine liver fibrosis recruits host effector cells improving fibrosis, regeneration, and function. Hepatology 53:2003–2015. https://doi.org/10.1002/hep.24315
34. Bansal R, Nagórniewicz B, Prakash J (2016) Clinical advancements in the targeted therapies against liver fibrosis. In: Mediators of inflammation. https://www.hindawi.com/journals/mi/2016/7629724/. Accessed 14 Jan 2018
35. Lefebvre E, Moyle G, Reshef R, Richman LP, Thompson M, Hong F, Chou HL, Hashiguchi T, Plato C, Poulin D, Richards T, Yoneyama H, Jenkins H, Wolfgang G, Friedman SL (2016) Antifibrotic effects of the dual CCR2/CCR5 antagonist Cenicriviroc in animal models of liver and kidney fibrosis. PLoS One 11:e0158156. https://doi.org/10.1371/journal.pone.0158156
36. Friedman SL, Ratziu V, Harrison SA et al (2018) A randomized, placebo-controlled trial of Cenicriviroc for treatment of nonalcoholic steatohepatitis with fibrosis. Hepatology n/a-n/a. https://doi.org/10.1002/hep.29477
37. Guicciardi ME, Trussoni CE, Krishnan A, Bronk SF, Lorenzo Pisarello MJ, O'Hara SP, Splinter PL, Gao Y, Vig P, Revzin A, LaRusso NF, Gores GJ (2018) Macrophages contribute to the pathogenesis of sclerosing cholangitis in mice. J Hepatol 69:676–686. https://doi.org/10.1016/j.jhep.2018.05.018
38. Krenkel O, Tacke F (2017) Liver macrophages in tissue homeostasis and disease. Nat Rev Immunol 17:306–321. https://doi.org/10.1038/nri.2017.11
39. Bartneck M, Warzecha KT, Tacke F (2014) Therapeutic targeting of liver inflammation and fibrosis by nanomedicine. Hepatobiliary Surg Nutr 3:364–376. https://doi.org/10.3978/j.issn.2304-3881.2014.11.02
40. Wang N, Liang H, Zen K (2014) Molecular mechanisms that influence the macrophage M1–M2 polarization balance. Front Immunol 5. https://doi.org/10.3389/fimmu.2014.00614
41. Eltzschig HK, Sitkovsky MV, Robson SC (2012) Purinergic signaling during inflammation. N Engl J Med 367:2322–2333. https://doi.org/10.1056/NEJMra1205750
42. Morganti JM, Riparip L-K, Rosi S (2016) Call off the dog(ma): M1/M2 polarization is concurrent following traumatic brain injury. PLoS One 11:e0148001. https://doi.org/10.1371/journal.pone.0148001